THE DEVELOPMENT OF GIANT RADIATING DIKE SWARMS ON VENUS FROM COUPLED MECHANICAL MODELS. Gerald A. Galgana[1], Patrick J. McGovern[1] and Eric B. Grosfils[2]; [1]Lunar and Planetary Institute, USRA, 3600 Bay Area Blvd., Houston, TX 77058; (galgana@lpi.usra.edu, mcgovern@lpi.usra.edu); [2]Geology Department, Pomona College, Claremont, CA 91711 (egrosfils@pomona.edu).

Introduction: Giant, centrally radiating fracture systems (interpreted as dikes) that extend several hundreds of kilometers from a central source are among the most prominent geologic structures found on the surface of Venus. The majority of these fracture systems are interpreted to be surface expressions of shallow, lateral dike injection from a central magmatic source [1]. Radiating dike systems on Venus are thought to originate through crustal response from sub-lithosphere processes of mantle upwelling, basal impingement, and then lateral expansion of mantle diapirs [1-6]. The formation of overlapping concentric dikes (or grabens), such as those found on some coronae and other volcanic structures, on the other hand, have been attributed to subsequent surface relaxation [e.g., 2-5] due to the withdrawal of magmatic material or deflation. A possible origin of these radial and concentric dikes, proposed by many authors, is propagation directly from shallow magma reservoirs [i.e., 7-9], but [10] shows that this is not actually a direct consequence of reservoir inflation and rupture as proposed, nor is it a consequence of edifice loading [11-12]. Numerous authors looking at crustal response to diapiric impingement have shown that uplift yields a surface stress field that is consistent with fracture patterns observed at the surface [e.g., 2-6]. However, these authors have not shown why magma ascending from depth into such a stress field will transition from vertical to lateral propagation, nor have they examined the impact on failure of a reservoir within the crust to ascertain whether lateral dike injection can occur directly from an inflating reservoir within the flexurally uplifting crust. Here, using Finite Element (FE) models, we examine the coupled effect of uplift and reservoir pressurization and its influence on reservoir failure modes. We then analyze the implications on dike formation, magma ascent and lateral propagation.

Models: We develop gravitationally loaded, axisymmetric FE models (with lithostatic prestresses) of the Venusian lithosphere, representing two thicknesses (T_e = 20 and 40 km; Lithosphere radius L_r = 900 km). Horizontal movement is constrained at the distal part of the model, while Winkler forces are imposed at the bottom of the lithosphere to simulate the effects of buoyant forces due to the lithosphere-asthenosphere density contrast. Uplift is represented initially by a 5 km thick by 200 km radius conical load (the initial stages of plume contact) and later by a disc-shaped (representing laterally spreading mantle diapirs) distributed load applied centered at the symmetry axis, with volume equivalent to the conical uplift.

Spherical magma chambers (r = 1 km, modeled as magma-filled cavities) are embedded in every model at different depths. These reservoirs are then incrementally pressurized to the point of failure; i.e., we interpret that failure occurs when component reservoir wall stresses (tangential (σ_T) or hoop (σ_θ)) reach tensile values (i.e, $\sigma = 0$). From these loading conditions, we predict fracture orientations and modes of magma intrusions; we also interpret the likelihood of magma ascent within the lithosphere based on the resulting stress magnitudes and the orientation of principal stress axes within the lithosphere.

Results: Our models with conical uplifts produce flexural "dipole" stress states with high differential stresses ($\sigma_D = \sigma_E - \sigma_C$, i.e., the most extensional stress minus the most compressional stress) at the upper and lower part of the lithosphere, separated by a low-stress neutral plane. Extension dominates the upper lithosphere, while the lower lithosphere is under compression. In the upper part, is σ_E oriented out of the model plane, while σ_C is vertical. In the lower lithosphere, σ_E is vertical while is σ_C is radial (horizontal). In contrast, thin lithosphere models incorporating disc-shaped diapirs predict stress states near the symmetry axis that approximate edifice-loaded models, with significantly lower differential stresses within the region surrounding a high stress area near the expanding magma chamber (Figure 1). Near the model center, at the upper part of the lithosphere, $\sigma_E = \sigma_v$ (vertical stress), while $\sigma_C = \sigma_r$ (radial or horizontal stress). Circumferential faulting is predicted at L_r~50 to 180 km ($\sigma_E = \sigma_r$, $\sigma_C = \sigma_v$). In comparison, $\sigma_E = \sigma_\theta$ and $\sigma_C = \sigma_r$ near the radial edge of the diapir load, at r ~180 to 230 km from the model center. At this outer region, the lithosphere has a pronounced flexed state with high σ_D region separated by a low σ_D. In comparison, thick lithospheres with disc uplift loads tend to have nearly similar stress patterns with conical loads.

Lithospheric stresses affect magma chamber failure modes: for models with conical uplift loads (or thick T_e with disc loads), reservoirs situated at the upper part of the lithosphere tend to fail near the crest, while those at the lower part tend to fail along the midsection. In thin lithospheres with disc uplift, magma reservoirs fail at the crest (Figure 2), while in thick lithospheres, sill-producing midsection failure occurs at depths > 20 km.

Discussion: We find that broad, disc-shaped uplift produces significantly different stresses and reservoir failure modes than conical uplift. However, as the lithosphere thickens, the sensitivity to uplift geometry decreases, producing comparable fractures due to nearly identical stress states. Our models can explain how evolving diapirs are responsible for variations in fractures found on Astra/Novae and Coronae as hypothesized in previous studies. In turn, the patterns of fractures found on Venusian volcanic centers may give hints about their evolution: initial domical rise produces radial fractures, while annular fractures may arise from the diapir's subsequent lateral expansion. For instance, the radial pattern of fractures found on Mbokomu Mons and Mokos suggest initial stages of uplift, precursory to the formation of circumferential fractures and building of the volcanic edifice. Circumferential grabens associated with radially propagating fractures found on Selu corona, Bhumidevi corona, and Miralaidji may be effectively explained by lithospheres uplifted by broad, disc-shaped mantle diapirs. In lithospheres with conical uplift, basal stresses produce a flexural stress state which promotes domical centers surrounded by radial fractures in the upper lithosphere while allowing sill-like horizontal fractures to develop at the lower region [i.e., 13]. Upper lithosphere reservoirs that tend to rupture near the crest may release magma upward through these radial fractures. However, magma chambers situated at the lower lithosphere region that tend to develop sill-like fractures tend to be stable at depth. In comparison, broad, disc uplifts create entirely different stress regimes that promote plateau-like central topographies. In such cases, concentric, circumferential fractures tend to form at the shallow lithosphere, a distance from the uplift center, complemented by radially-oriented fractures at the outermost boundary of the load.

We are continuing to investigate how magma can roll over from initial vertical ascent, and be channeled laterally through radiating fractures, hundreds of kilometers away from their central sources. This may occur when magma driven by overpressured shallow reservoirs is horizontally directed by edifice-driven compressive stresses. When magmatic pressures exceed fracture-normal compressive stresses exerted by the lithosphere, crack propagation occurs, followed by injection and lateral spread of magma from the central source [14-15]. Compressive "stress traps", which arise from increasing volcanic loads in the upper lithosphere, leave a subsurface stress state that favors radial dike propagation and further directs lateral propagation of magma intrusions [i.e., 11, 16]. While other authors have argued that buoyant forces will dominate and result in dike propagation [e.g., 17], our models explain the necessary mechanical link between flexural stress states, highly pressurized reservoirs, the initial rupturing process and magma ascent. We continue to explore volcanologically plausible ways to explain direct lateral magma propagation from the magma chamber to regions far from the chamber, where our models predict radially propagating intrusions should be favored.

References: [1] Grosfils, E. and J. Head (1994) *GRL,* 21(8): 701-704. [2] Stofan, E. et al. (1992) *JGR*, 97:13,347-13,378. [3] Koch D. and M. Manga (1996) *GRL*, 99:225-228. [4] Krassilnikov, A. and J. Head (2003) *JGR,* 108(E9), 5108. [5] Janes, D. and S. Squyres (1993) *GRL* 20(24):2,961-2,964. [6] Cyr, K. and H. Melosh (1993) *Icarus*, 102:175-184. [7] Parfitt, E. et al. (1993) *JVGR*, 55(1-2). [8] Koenig, E. and D. Pollard (1998) *JGR*, 103(B7): 15,183-15,202. [9] McLeod, P. and S. Tait (1999) *JVGR*, 92:231-245. [10] Grosfils, E. (2007) *JVGR*, 166: 47-75. [11] Hurwitz, D., et al. (2009) *JVGR*, 188:379-394. [12] Galgana, G. et al. (2010) *JGR*, doi:10.1029/2010JE 003654, in press. [13] Galgana, G. et al. (2010) *LPSC XLI*, 1777. [14] Rubin, A. (1993) *JGR*, 98:15,919-15,935. [15] Rubin, A. (1995) *Annu. Rev. Earth Planet. Sci.* 23:287-336. [16] McGovern, P. and S. Solomon (1993) *JGR*, 98: 23,553-23,579. [17] Lister, J. and R. Kerr (1991) *JGR* 96: 10,049-10,077.

Figures

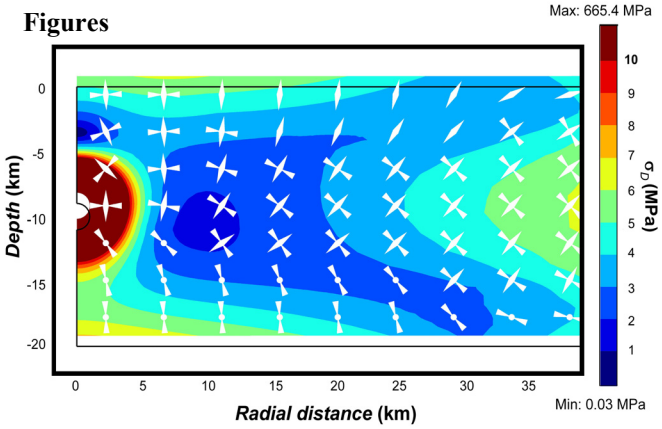

Figure 1. Cross-section of axisymmetric model with disc uplift (Depth to reservoir D_{tC} = 10 km, T_e = 20 km, x,y axes in km). Colors correspond to differential stresses (red = high, blue = low, units in MPa). Arrows represent principal stress axes (Arrows pointing inwards = compression; arrows pointing outwards = extension; dots = out of plane). Black outline shows undeformed lithosphere.

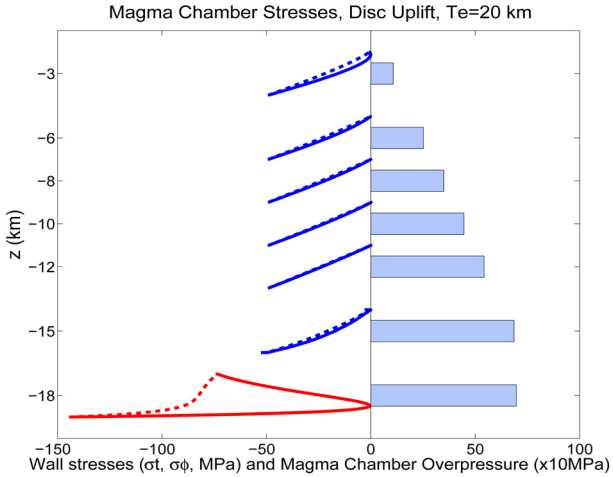

Figure 2. Tangential stresses (σ_t, solid lines) and circumferential stresses (σ_θ, dashed lines) along magma chamber wall, for models at various with *DtC*s (blue curves = near-crest failure; red curves = near-midsection failure, units in MPa, z = depth in km). Horizontal Bars = maximum pressurization at tensile failure (i.e., σ_t or $\sigma_\theta = 0$, units in tens of MPa).